Charged-pion production in noninclusive proton-nucleus interactions at 0.8 and 1.6 GeV incident energies

M.-C. Lemaire,[1,2,*] M. Trzaska,[1,†] J. P. Alard,[3] J. Augerat,[3] D. Bachelier,[4] N. Bastid,[3] J.-L. Boyard,[4] C. Cavata,[1] P. Charmensat,[3] P. Dupieux,[3] P. Gorodetzky,[5] J. Gosset,[1] T. Hennino,[4] J.-C. Jourdain,[4] A. Le Merdy,[1] D. L'Hôte,[1] B. Lucas,[1] J. Marroncle,[3,‡] G. Montarou,[3] M.-J. Parizet,[3] J. Poitou,[1] D. Qassoud,[3] P. Radvanyi,[2] B. Ramstein,[4] A. Rahmani,[3] M. Roy-Stephan,[4] O. Valette,[1] P. Zupranski,[2] J. Cugnon,[6] and J. Vandermeulen[6]

[1]*Department de Physique Nucléaire, Centre d'Etudes Nucleaires de Saclay, 91191 Gif-sur-Yvette CEDEX, France*

[2]*Laboratoire de Nucléaires Sciences, Centre d'Etudes Nucléaires de Saclay, 91191 Gif-sur-Yvette CEDEX, France*

[3]*Laboratoire de Physique Corpusculaire, Clermont-Ferrand, Boite Postale No. 45, 63170 Aubière, France*

[4]*Institut de Physique Nucléaire, Orsay, Boite Postale No. 1, 91406 Orsay, France*

[5]*Centre de Recherches Nucléaires, Boite Postale No. 20 CR, 67037 Strasbourg CEDEX, France*

[6]*Liège University, B-4000 Sart Tilman, Belgium*

(Received 13 November 1990)

Charged pions and light nuclei (p, d, t, ^{3}He, and ^{4}He) have been measured in the interaction of proton beams with C, Nb, and Pb targets at 0.8 and 1.6 GeV incident energies, using a large solid angle detector. From slices on the multiplicity of protonlike particles (free protons and protons bound in light fragments), the events have been sorted out into two classes corresponding to more peripheral and more central collisions. For each class of events, the mean value and the dispersion of the π^+ and π^- multiplicity distributions have been studied as a function of target mass and incident energy. Comparisons to the Liege intranuclear cascade predictions exhibit some discrepancies which are discussed.

I. INTRODUCTION

Pion production in both proton-nucleus (pA) and nucleus-nucleus (AA) collisions is an important subfield of intermediate-energy nuclear physics. In nucleus-nucleus collisions, the major goal is to obtain information on the behavior of nuclear matter at finite temperature and high densities with the hope that the nuclear equation of state (EOS) may be determined. The knowledge of the EOS is very important in connection with the models developed to describe supernovae explosions[1] and, more generally, in any theory of nuclear dynamics.

The problem is to find experimental observables that represent signatures of the high-density and high-temperature stage. Some years ago, pion multiplicity was proposed[2–5] for being such an observable. It has even been used to extract an EOS via the excitation function of the pion yield.[3,4] Intranuclear cascade calculations (INC) were indeed predicting too large pion yields, and the difference was ascribed to the lack of compression energy in the model. Later on, simulations with the Boltzmann-Uehling-Uhlenbeck (BUU) model[6,7] showed that, even though the introduction of a nuclear mean field lowers the number of produced pions toward the experimental value, the absolute yield remains too high. Then, Gale[8] found that by introducing the momentum dependence of the interaction in the BUU model, the experimental pion multiplicity excitation function could be reproduced between 0.36 and 1.8 GeV/nucleon, but no difference between soft and stiff EOS could be pointed out. Similarly, Aichelin *et al.*[9] demonstrated in the framework of quantum molecular dynamics (QMD) that momentum-dependent nuclear interactions suppress pion yields much more than hard local potentials. However, they also mentioned that these results should be taken with caution since no density or temperature renormalization of the nucleon-nucleon interaction was taken into account. There is no doubt about the change of the elementary cross sections by the nuclear medium,[10–13] but there is not yet a clear answer about how it will affect the nucleus-nucleus data as this effect has only been tested quite crudely by changing globally the cross sections[8,14] without local density dependence.

In order to check the ingredients of these transport theories, it is important to have proton-nucleus data. Extensive measurements of inclusive pion production in pA collisions now exist between 0.2 and 1 GeV incident energies.[15–19] However, because of impact parameter averaging, such experimental information has its maximum weight for peripheral collisions and cannot provide a valid test of what would be the influence of any density-dependent force. The aim of the present work was to get information on the pion production in proton-nucleus collisions together with a criterion which allows the selection of the density. To achieve this goal, both π^+ and π^- multiplicities were measured with selections on the multiplicity of protonlike particles (free protons and protons bound in light composites) in order to distinguish between peripheral and nonperipheral collisions.

In Sec. II, the experimental layout and data reduction procedure are described. As the INC calculations used for comparison to the experimental data strictly follow the procedure given in Ref. 14, a very short summary will be given in Sec. III. Measured multiplicities of proton-

like particles and charged pions are reported in Sec. IV and compared to INC predictions. Special interest will be devoted to a comparison with similar exclusive measurements performed with the same DIOGENE detector,[20] but with α beams,[21–23] for which discrepancies between the data and INC predictions could not be attributed clearly either to a failure of the INC calculations or to compression effects.

II. EXPERIMENTAL SETUP AND DATA REDUCTION PROCEDURE

A. Experimental layout

The experiment was performed at the SATURNE II synchrotron in Saclay with the pictorial drift chamber (PDC) of the DIOGENE large solid-angle detector, a complete description of which can be found in Ref. 20.

The PDC is 80 cm long and 70 cm in diameter; it is located inside a solenoid delivering a magnetic field of 1 T parallel to the beam direction. Tracks may be measured between 8.4 and 33.7 cm from the beam axis with at most 16 sample points. From each of them, one determines the three spatial coordinates and energy loss. Typical values of the resolutions for pions and protons are about 20% [full width at half maximum (FWHM)] for the momentum and a few degrees for the azimuthal angle θ and the polar angle ϕ. The PDC surrounds a 2-mm-thick, 10-cm-diam carbon-fiber beam pipe. The acceptance of the detector is limited by the fact that the emitted particles must have enough energy to cross the target and beam pipe; it depends also, of course, on the number of wires required to analyze a track. To have clean cuts, the acceptance used for the data analysis has been imposed by software to be more restrictive than the raw experimental one (see Sec. II B).

The trigger system consisted of four scintillators. The first detector S1, located 3.52 m upstream from the target, counts each beam particle; it is 1 mm thick, 30 mm in diameter. Two 10-mm-thick scintillators AH1 and AH2, each having a 15-mm-diam central hole, were used to reject the beam halo and particles produced by reactions in S1. They were placed 0.33 and 1.56 m downstream of S1. As opposed to the description of Ref. 20, in the present measurement the scintillator beam veto (BV) counter was located 3.75 m downstream of the target. It was a square of 100×100 mm^2 area, 1 cm thick. The fast trigger signal was given by $\mathrm{S1}\cdot\mathrm{AH1}+\mathrm{AH2}\cdot\overline{\mathrm{BV}}\cdot\overline{\mathrm{TM}}$, where TM is the dead time. This trigger implied that an interaction occurred in the target. The timing was always given by S1. A second-level trigger that required that at least one charged particle reach a radius of 15 cm from the beam axis was performed in the acquisition program. The dead time was about 30% for a proton-beam intensity of a few 10^5 particles per spill, with spills of about 500 ms every 1.4 s at 800 MeV or every 1.8 s at 1.6 GeV.

The target was located 20 cm upstream from the center of the PDC. We used disks of about 5–6 mm diameter, with thicknesses of, respectively, 1.79 g/cm^2 for C, 1.86 g/cm^2 for Nb, and 1.24 g/cm^2 for Pb. These disk shapes of the targets were chosen in order to minimize the energy loss of particles emitted at 90° and to keep a good quality of the track reconstruction program. However, as the beam diameter is larger than the target one, special runs with both large-diameter targets and empty targets had to be done to get absolute cross sections, with $\pm$ 15% accuracy. Special care has been devoted to control run by run that the beam conditions were stable.

The total number of recorded events was about 10^6 events for each target at both energies, with only half of it for the C target run at 1.6 GeV.

B. Data reduction procedure

The PDC calibrations were done as described in Ref. 20. The time pedestals for all wires, as well as drift angle and drift velocity, were found to be relatively stable over the whole set of runs. In contrast, the energy-loss calibration varied quite strongly from run to run because of a gas leak in the detector. Therefore, gain factors had to be adjusted run by run in order to keep the same particle identification criteria in the reconstruction program RATRADI.[24] The π-p-d separation is very good. From the analysis of Ref. 23 and our identification spectra, the data are not spoiled by contamination of the measured pions by the electrons and positrons which are created by gamma-ray conversion inside the target and beam pipe.

The RATRADI program has been used for the track reconstruction, particle identification, and computation of each particle's momentum vector and associated uncertainties. From complete simulations of the detector, including the effects of the electronic biases and the reconstruction program, it was found that inefficiencies due to multitrack separation are negligible for multiplicities smaller than ~ 10.

Even though it has a large acceptance, DIOGENE detector does not detect particles emitted at forward and backward polar angle θ or particles with low kinetic energies. The software acceptance cuts are chosen to be more restrictive than the raw experimental ones[20] to assure that at least nine hits are measured for each track (in order to get a good identification) and to get rid of the particles detected with momentum resolution $\geq 20\%$ (FWHM). As in the present experiment, the 2-mm-thick carbon-fiber tube has been used, the parametrizations of the cuts in the $(y,p_\perp/m)$ plane (y being the rapidity and $p_\perp/m$ being the transverse momentum divided by the mass of the particle) have been revised.[25] As many models do not produce light composite fragments, we have to define "protonlike" (p_{like}) particles. It corresponds to the sum of protons free or bound in light composite fragments:

$$M(p_{\mathrm{like}})=M(p)+M(d)+M(t)+2[M(^3\mathrm{He})+M(^4\mathrm{He})]\ . \tag{1}$$

With this prescription, a protonlike particle bound in a deuteron, for example, has the same velocity and emission angle as the deuteron itself. Then the analysis is performed in the following way.

An event is accepted if at least one charged particle (among p_{like}, π^+, or π^-) satisfies the trigger acceptance cuts

$$24^\circ \leq \theta \leq 128^\circ ,$$

and for a pion:

$$p_\perp/m \geq \begin{cases} 0.60+1.29y & (\text{if } y<0) \\ 0.60-0.96y & (\text{if } y \geq 0) , \end{cases} \tag{2a}$$

and for a baryon

$$p_\perp/m \begin{cases} 0.24+0.47y & (\text{if } y<-0.032) \\ 0.286 & (\text{if } -0.032 \leq y<0) \\ 0.24-0.62y & (\text{if } y \geq 0) . \end{cases} \tag{2b}$$

For each accepted event, a pion or a protonlike particle is taken into account in the analysis if it is in the polar angular range

$$20^\circ \leq \theta \leq 132^\circ$$

and satisfies the detector acceptance cuts, which, in the $(y,p_\perp/m)$ plane, are taken identical to those defined above as the trigger acceptance cuts.

III. INC SIMULATIONS

The version of the Liege intranuclear cascade code used for the present calculations has been largely described in Ref. 14 and references therein. Trapezoidal shapes of the nuclear density profile have been used to take into account the nucleus diffuse edge. The nucleon momenta of the target nucleons are distributed initially at random inside a sharp Fermi sphere of radius 270 MeV/c. The nucleons move along straight-line trajectories until the minimum relative distance between two of them becomes smaller than the strong-interaction radius between two nucleons. The final momenta of the particles are determined at random, in agreement with conservation laws and experimental cross sections. Inelasticity is taken into account through Δ excitation. In this version the Δ has a finite lifetime so that it can decay during the collision. The isospin dependence of the cross sections is included. The spectator nucleons are frozen. The binding potential V encountered by a target nucleon is implemented in the following way (Cahay, Cugnon, and Vandermeulen[2]): at the first collision, the energy-momentum relation

$$E^2=p^2+(m+V)^2$$

has to be satisfied. Once the nucleon has made a collision, the average field is destroyed. The values of V are taken, respectively, equal to -25 MeV for C and -40 MeV for Nb and Pb targets, in agreement with analysis of Monitz *et al.* of quasielastic electron-scattering data.[26] The Pauli blocking factor is calculated in a way similar to what is done in BUU and VUU codes. For each event the occupation factor f is determined by examining the neighborhood of the final-state phase space whenever a collision would otherwise occur. The nucleons are counted in a sphere centered at the final phase-space coordinates of the colliding pair. The sphere has a radius of 2 fm in coordinate space and 200 MeV/c in momentum space.

At seven values of impact parameter between 0 and the maximum value, b_{max}, 10 000 (3500 and 2000) events were simulated for the C (Nb and Pb) target at both 0.8 and 1.6 GeV incident energy. The total cross sections of the INC simulations were found, respectively, to be equal to 324, 1158, and 1846 mb for C, Nb, and Pb targets. For carbon these values agree fairly well with the experimental values of Jaros *et al.*:[27] 364.7 and 377.5 mb, respectively, at 0.87 and 2.1 GeV incident energies. Ray[28] found 1650 mb for $p+$Pb at 0.8 GeV.

IV. RESULTS

A. Protonlike multiplicity distributions

The data measured on the three targets C, Nb, and Pb are displayed in Figs. 1 and 2, respectively, for 0.8 and 1.6 GeV incident energies. A comparison to INC predictions is also shown. The INC protonlike integrated cross sections agree with the experimental ones within 10%. The mean multiplicities are listed in Table I. For the target mass dependence, one observes an increase of the mean multiplicity from C to Nb, but no change from Nb to Pb. For the incident energy dependence, there is no change for the C target, but an increase of about 30% for Nb and 40% for Pb between 0.8 and 1.6 GeV. This energy dependence can be understood in the following way. For the C target, the number of nucleons involved in the collisions is limited. Therefore, one can expect that with increasing incident energies there is no increase of protonlike particles emitted at large angles with a sufficient kinetic energy to overpass the experimental energy cuts. In contrast, for a heavy target the number of cascading nucleons is larger so that the number of measured protonlike particles emitted at large angles with sufficient kinetic energy might be an increasing function of the incident energy. The INC calculations generally overpredict the cross sections for large multiplicities, the discrepancies between experimental and theoretical

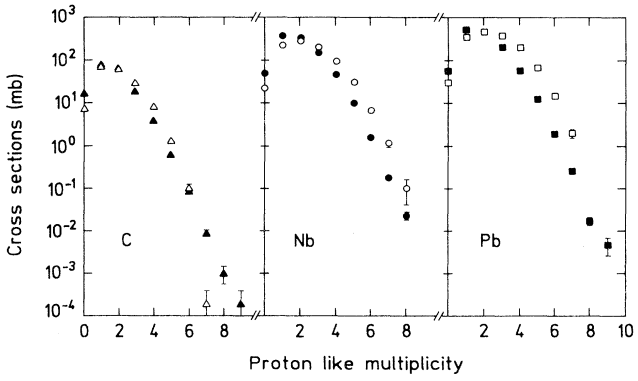

FIG. 1. Cross section versus protonlike multiplicity (see Sec. II B) for the interactions of 0.8-GeV protons with C (triangles), Nb (circles), and Pb (squares) targets. The experimental data (solid symbols) are compared to the cascade predictions (open symbols).

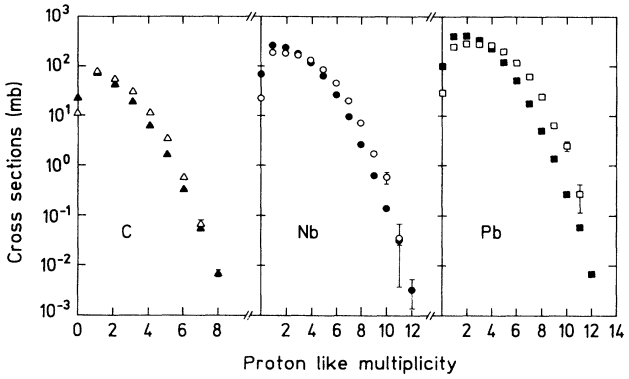

FIG. 2. Same as Fig. 1 for the interactions of 1.6-GeV protons with C (triangles), Nb (circles), and Pb (squares) targets.

values being larger for heavier targets. The experimental dependences upon target mass, incident energy, and the differences between experimental results and INC predictions are consistent with the previous finding from α-nucleus studies.[21] There are large differences between theory and experiment for large multiplicities and for heavy targets, even though the present INC code was improved by inclusion of the binding potential V and has a more realistic description of the nuclear surface.

B. Impact parameter selection

The relationship between impact parameter and protonlike multiplicity has been studied through INC simulations. The results are displayed in Figs. 3–5 and Tables II and III. From these calculations, it is clear that taking a protonlike multiplicity strictly equal to 1 selects large values of the reduced impact parameter b_r ($b_r = b/b_{\max}$), on the average about 0.7 for C target and 0.8 for Nb and Pb targets. These events will be taken as characterizing "peripheral" collisions. A selection of events with larger protonlike multiplicities always restricts b_r to about 0.5. Increasing the multiplicity threshold does not change the impact parameter selection, but just reduces the number of events. The correspondence between the multiplicity selection and fraction of geometrical cross section is also given in Tables II and III for the experimental results. "Central" collisions will be taken towards the highest multiplicity representing about 20% of the geometrical cross section. The corresponding multiplicity selections are $M > 1$ for C and $M > 2$ for Nb and Pb targets at 0.8

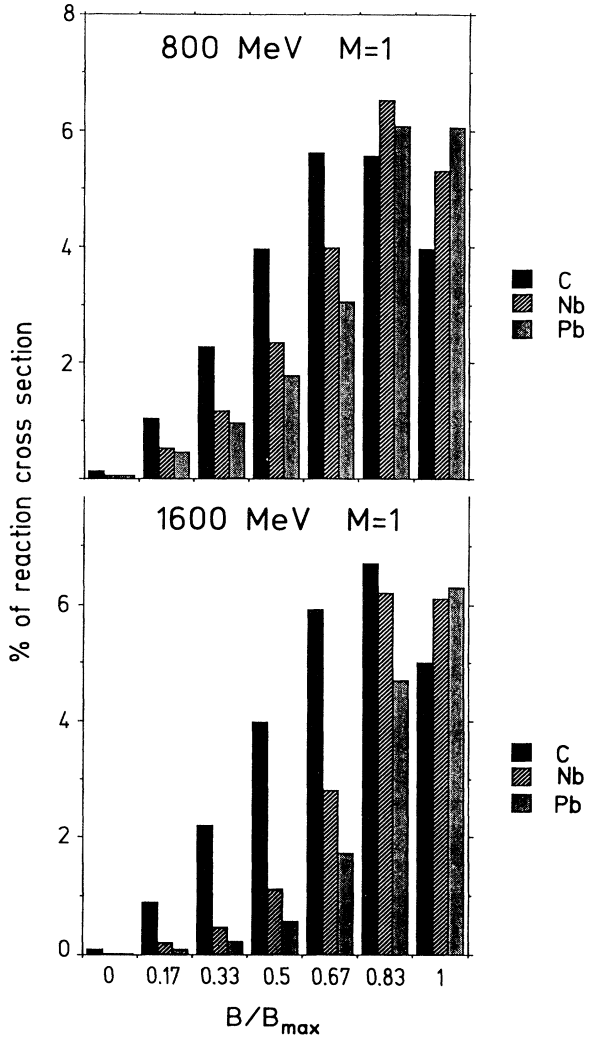

FIG. 3. Impact parameter distribution for INC events with a detected protonlike multiplicity equal to 1 for proton interaction with C (solid bars), Nb (hatched), and Pb (dotted) targets at 0.8 (top) and 1.6 (bottom) GeV incident energies.

GeV, and $M > 1$ for C, and $M > 3$ for Nb and Pb at 1.6 GeV. Because of the fact that the experimental protonlike multiplicity distributions are not perfectly reproduced by the INC model, the same multiplicity thresholds in the experimental data and INC simulations do not

TABLE I. Experimental and predicted (INC) mean values of the protonlike multiplicity. The ratio R_1 between predicted and experimental values is also indicated.

Incident energy	800 MeV			1600 MeV		
Target	C	Nb	Pb	C	Nb	Pb
Expt.	1.53±0.001	1.81±0.001	1.78±0.001	1.51±0.001	2.39±0.002	2.53±0.002
INC	1.79±0.003	2.26±0.007	2.42±0.008	1.83±0.004	2.93±0.011	3.37±0.015
R_1	1.17±0.005	1.25±0.009	1.36±0.026	1.21±0.011	1.22±0.031	1.33±0.047

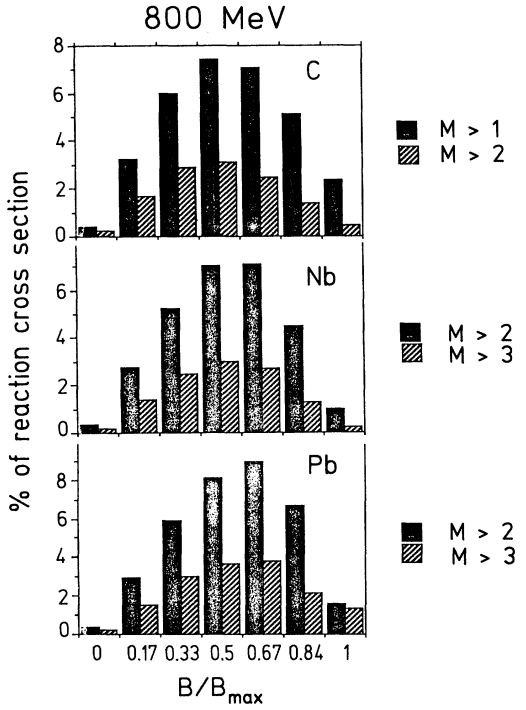

FIG. 4. Impact parameter distribution of INC events with various conditions on the protonlike multiplicity M, defined on the right edge of each figure, for proton interactions with C, Nb, and Pb targets at 0.8 GeV incident energy.

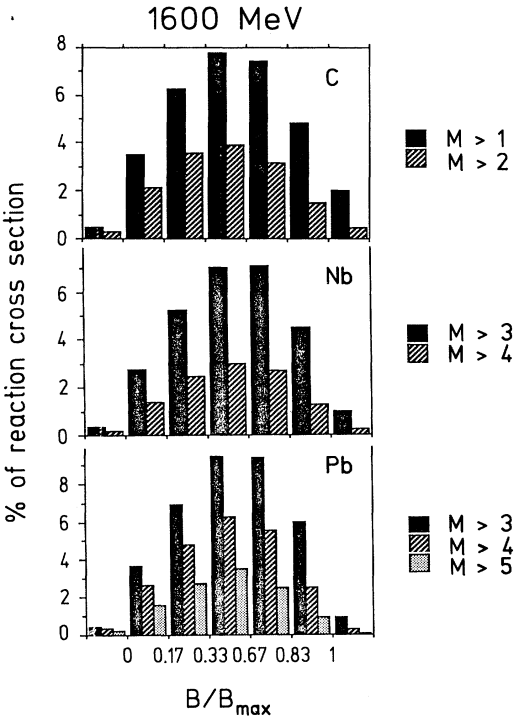

FIG. 5. Same as Fig. 4 for proton interactions with C, Nb, and Pb targets at 1.6 GeV incident energy.

TABLE II. Percentage F of the reaction cross section with various conditions on the protonlike multiplicity M, for experimental results (F_{expt}) and INC simulations (F_{INC}), in 0.8-GeV proton interactions with C, Nb, and Pb targets. For INC simulations the mean value of the reduced impact parameter $b_r = b/b_{\max}$ is also indicated (uncertainty of ± 0.05).

		800 MeV		
Target	M	F_{expt}	F_{INC}	$b/b_{\max}$
C	1	26	22	0.7
Nb	1	30	20	0.7
Pb	1	28	18	0.8
C	>1	27	32	0.6
	>2	7	12	0.5
Nb	>2	17	28	0.5
	>3	5	11	0.5
Pb	>2	14	35	0.6
	>3	4	15	0.6

correspond exactly to the same fraction of the geometrical cross section, as can be seen from Tables II and III.

C. Pion multiplicities

1. *Mean multiplicities*

The mean multiplicities of charged pions measured at the two energies 0.8 and 1.6 GeV are displayed as a function of target mass in Fig. 6 for peripheral collisions and Fig. 7 for central collisions. They are compared to INC predictions.

a. Peripheral collisions. From Fig. 6 it can be seen that, with increasing target mass, at 0.8 GeV the mean multiplicity of positive pions decreases by about a factor of 2 between C and Pb, while the mean multiplicity of negative pions stays roughly constant. These results are similar to those obtained in α-nucleus reactions measured at 0.8 GeV/nucleon.[22,23] A weak target mass dependence of π^- means multiplicity for light projectiles was also found in experiments performed with the Dubna bubble chamber[29] at 3.36 GeV/nucleon. In this case, as well as for inclusive data, one expects a major contribution from

TABLE III. Same as Table II for 1.6-GeV proton interactions with C, Nb, and Pb targets.

		1600 MeV		
Target	M	F_{expt}	F_{INC}	$b/b_{\max}$
C	1	24	25	0.7
Nb	1	24	17	0.8
Pb	1	22	14	0.9
C	>1	23	32	0.5
	>2	9	13	0.5
Nb	>3	20	26	0.5
	>4	9	14	0.5
Pb	>3	23	37	0.5
	>4	11	22	0.5
	>5	4	12	0.5

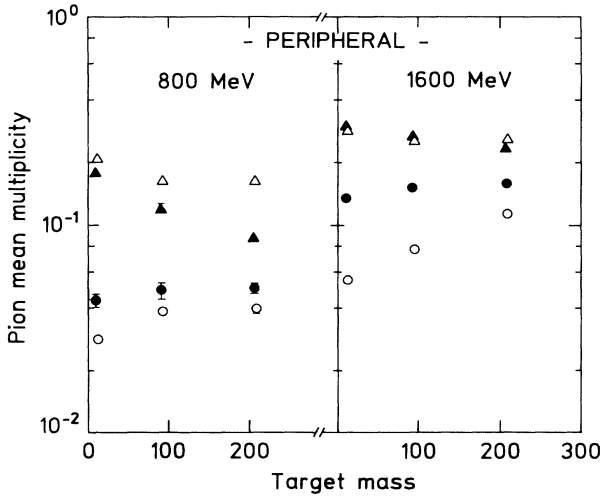

FIG. 6. Mean pion multiplicity versus target mass, for peripheral (see Sec. IV B) interactions of protons at 0.8 (left) and 1.6 (right) GeV incident energies. Solid (open) symbols correspond to experimental results (INC predictions), triangles (circles) to positive (negative) pions.

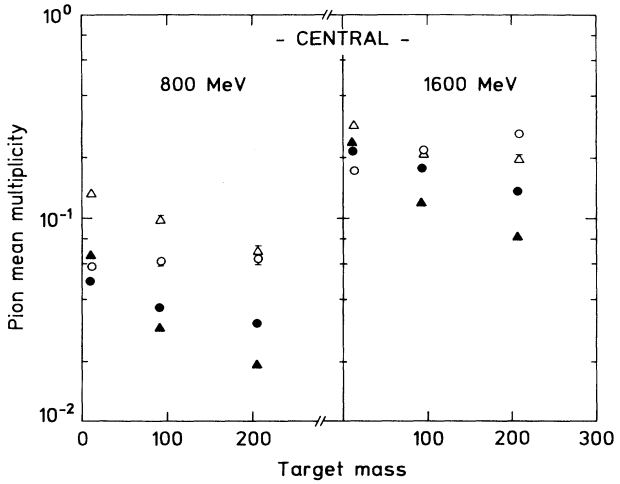

FIG. 7. Mean multiplicity of π^+ (triangles) and π^- (circles) versus target mass, for central (see Sec. IV B) interactions of 0.8 (left) and 1.6 (right) GeV protons with C, Nb, and Pb targets. Solid and open symbols correspond to experimental results and INC predictions, respectively.

the peripheral collisions due to the $2\pi b$ db weight. The inclusive data of Cochran *et al.*[15] and Crawford *et al.*[16] show that the pion cross sections vary as

$$\sigma(\pi^+)=\alpha(Z_T)^{1/3},\quad \sigma(\pi^-)=\beta(N_T)^{2/3}\ , \tag{3}$$

where α and β are constants, and Z_T and N_T are, respectively, the target proton and neutron numbers. Such a behavior was explained by the fact that the π^+ production is essentially coming from the first proton-proton collision, leading to a Δ excitation and decay. In contrast, the π^- production process is more complicated than expected from the isobar model, an important source coming from the $\pi^0+n\rightarrow\pi^-+p$ charge-exchange reaction so that the π^- production cross section is proportional to the nuclear area times (N_T/A_T), where A_T is the target mass, or roughly proportional to $(N_T)^{2/3}$. As the total reaction cross section varies as $(A_T)^{2/3}$, one expects the following dependences of the pion multiplicities:

$$\begin{aligned} M\langle\pi^+\rangle &\approx (Z_T)^{1/3}/(A_T)^{2/3}\ , \\ M\langle\pi^-\rangle &\approx (N_T)^{2/3}/(A_T)^{2/3}\ . \end{aligned} \tag{4}$$

The Nb-to-C and Pb-to-Nb ratios of pion multiplicities calculated with the preceding formulas and extracted from the experiment are compared in Table IV for both pion charges. At 0.8 GeV the experimental decrease of the π^+ mean multiplicity from C to Nb is slightly smaller than the predicted one; in contrast, both the decrease of the π^+ mean multiplicity observed between Nb and Pb targets and the independence of the π^- mean multiplicity with A_T are consistent with the trend given by Eq. (4). The deviation observed for the C-to-Nb ratio is expected since Eq. (4) was found to be satisfied only for $A \geq 27$ in $p + A_T$ interactions.[15,16]

At 1.6 GeV the π^+ mean multiplicity exhibits a smaller decrease with target mass: 30% from C to Pb instead of a factor of 2 at 0.8 GeV. The π^- mean multiplicity stays roughly constant with A_T within the error bars. This target mass dependence of the pion multiplicities is consistent with Eq. (4).

The ratios between INC predicted and experimental values of the mean pion multiplicities are listed in Table V. At 0.8 GeV the INC calculations overestimate the π^+ mean multiplicity from 20% for a C target up to about a factor of 2 for a Pb target. Such a behavior has also been observed in the analysis of the inclusive data.[14] The π^- mean multiplicities are underestimated, the effect being

TABLE IV. Ratios of pion mean multiplicities for different targets. The values estimated by formula (4) in Sec. IV C are compared with experimental ones.

	Nb/C			Pb/Nb		
	Eq. (4)	Expt 0.8 GeV	Expt 1.6 GeV	Eq. (4)	Expt 0.8 GeV	Expt 1.6 GeV
π^+	0.48	0.67	0.90	0.74	0.71	0.87
π^-	1.08	1.08	1.12	1.05	1.02	1.05

TABLE V. Ratio between INC prediction and experimental value of the pion mean multiplicities for peripheral collisions.

Incident energy		800 MeV			1600 MeV	
Target	C	Nb	Pb	C	Nb	Pb
π^+	1.17±0.03	1.36±0.07	1.90±0.11	0.95±0.05	0.95±0.05	1.11±0.07
π^-	0.64±0.05	0.79±0.09	0.80±0.10	0.40±0.02	0.51±0.05	0.72±0.08

the largest for the lightest target as it rises from 20% for Pb to 40% for C. At 1.6 GeV the π^+ mean multiplicity is well reproduced by the INC model for all targets. The π^- mean multiplicities are systematically underestimated, and like at 0.8 GeV, the discrepancy between the calculated and experimental values is the largest for the lightest target. It is interesting to study how these values can be compared with a simple model, assuming a single collision and that π production follows isobar dominance; then

$$M\langle\pi^+\rangle=\frac{5Z_T\sigma_{\text{in}}(pp)+N_T\sigma_{\text{in}}(np)}{6[Z_T\sigma_T(pp)+N_T\sigma_T(np)]}$$
$$M\langle\pi^-\rangle=\frac{N_T\sigma_{\text{in}}(np)}{6[Z_T\sigma_T(pp)+N_T\sigma_T(np)]}\ , \tag{5}$$

where $\sigma_{\text{in}}(pp)$ and $\sigma_{\text{in}}(np)$ are, respectively, the pp and np total inelastic cross sections, and $\sigma_T(pp)$ and $\sigma_T(np)$ are the pp and np total cross sections. Their values are, respectively, 6 mb for $\sigma_{\text{in}}(pp)$, 12 mb for $\sigma_{\text{in}}(np)$, 40 mb for $\sigma_T(pp)$, and 36 mb for $\sigma_T(np)$ at 0.8 GeV and become 20 mb for $\sigma_{\text{in}}(pp)$, 16 mb for $\sigma_{\text{in}}(np)$, 40 mb for $\sigma_T(pp)$, and $\sigma_T(np)$. The values found with the simple relationships (5) are compared to the experimental and INC values in Table VI. It is striking that there is a fairly good agreement between this simple Δ dominance model and INC calculations except for π^- mean multiplicities at 1.6 GeV. Both INC calculations and the Δ dominance model give too large π^+ multiplicities for the Pb target at 0.8 GeV, which can be understood as a lack of π absorption in the models. For π^- at 0.8 GeV, the INC calculations agree with the simple isobar model expectations, giving too low theoretical mean multiplicities as compared to the measured ones for C target. For the Pb target, the Δ dominance model underestimates the experimental mean multiplicity by about 70%, the INC calculations being closer to the experimental values; this feature might result from the large contribution of the π^0 charge-exchange reaction stated above. At 1.6 GeV the Δ dominance model underestimates the π^- mean multiplicities; INC calculations have also this tendency, except that the discrepancies with the experimental values are smaller. Then it is quite clear that the hypothesis of a single collision with π production through Δ dominance is too naive to explain π^- mean multiplicities. As pointed out by Sternheim and Silbar,[30] to reproduce both the (π^+, π^-) inclusive experimental cross sections and π^+/π^- cross-section ratios measured in p-nucleus collisions,[15] it is necessary to take into account, in addition to the isobar model, a good description of pion absorption and the π^0 charge-exchange reaction. They also mentioned that a correct treatment of the nuclear surface might be important.

Experimental and INC π^+/π^- multiplicity ratios are compared in Table VII. It clearly establishes the failure of the model when impact parameter selection is performed, as the calculations overestimate the experimental values by about a factor of 2 for all targets. It is interesting to note that the π^+/π^- inclusive cross-section ratios found by Cochran *et al.*[15] at 730 MeV are, respectively, 5.3 and 1.95 for the C and Pb targets, values which are closer to our experimental values than the INC predictions. For "peripheral" collisions, experimental π^+/π^- multiplicity ratios are not well described by INC calculations. For the inclusive cross sections,[14] it was found that, in the case of heavy targets, the absolute cross sections were overestimated by the calculations for both π^+ and π^-, but the ratios were in satisfactory agreement with the experimental values. These differences between results from peripheral collisions and inclusive measurements are not completely understood. They might result from the fact that we are dealing with a more restrictive region of the pion phase space, larger angles, and kinetic

TABLE VI. Experimental and predicted pion mean multiplicities for peripheral collisions. The calculated values are given for INC simulations (INC) and Δ dominance model (Δ).

Incident energy		800 MeV			1600 MeV	
Target		C	Nb	Pb	C	Nb	Pb
	Expt	0.179	0.120	0.086	0.298	0.267	0.233
π^+	INC	0.209	0.164	0.163	0.282	0.252	0.258
	Δ	0.20	0.18	0.17	0.24	0.22	0.21
	Expt	0.043	0.048	0.049	0.132	0.148	0.156
π^-	INC	0.028	0.038	0.039	0.053	0.075	0.112
	Δ	0.026	0.029	0.032	0.033	0.037	0.040

TABLE VII. π^+/π^- ratio of mean multiplicities for peripheral collisions: experimental values, INC predicted values, and ratio R_7 between INC and experimental values.

Incident energy	800 MeV			1600 MeV		
Target	C	Nb	Pb	C	Nb	Pb
Expt	4.16±0.08	2.50±0.06	1.75±0.03	2.26±0.03	1.80±0.03	1.49±0.03
INC	7.46±0.52	4.32±0.51	4.18±0.55	5.32±0.28	3.36±0.37	2.30±0.30
R_7	1.79±0.13	1.73±0.21	2.39±0.32	2.35±0.12	1.87±0.21	1.55±0.20

energies, in addition to the selective trigger condition (see Sec. II B) which, for all cases presently studied, corresponds to a total number of nucleon-nucleon collisions in the cascade process larger than 3.

b. Central collisions. Results on the mean multiplicities are displayed in Fig. 7, the corresponding values being listed in Table VIII. For "central" collisions there is a clear decrease of the π^+ mean multiplicity with the target mass. The A_T dependence of the π^- mean multiplicity displays the same behavior. These features are consistent with the results obtained in α-nucleus central collisions.[22] The decrease with target mass is weaker for negative than for positive pions, but it does not depend on the incident energy.

From the INC simulations, it has been checked that the mean pion multiplicity does not depend on the choice of the more or less restrictive multiplicity conditions defined in Sec. IV B and Tables II and III. The comparisons to the INC predictions displayed in Fig. 7 are quantitatively expressed in Table IX with the ratio R(INC/expt) between the π mean multiplicities calculated with the cascade model and the experimental values for both pion charges produced by interaction of the 0.8- and 1.6-GeV protons on the different targets. It is clear that the π^+ mean multiplicities are always overestimated by the INC calculations; the differences between the experimental and calculated values are the larger at the lower incident energy and for heavier targets. For π^- mean multiplicities, INC calculations describe fairly well the carbon data, while they overestimate the Pb data. It confirms the previous assumptions according to which the discrepancies observed between the INC and experimental data for pion production result mainly from the lack of pion absorption in the model.[14] It is interesting to note that the target mass dependence of R(INC/expt) does not depend on incident energy. For α-nucleus central collisions,[22] it has been shown that there is a linear dependence of $\ln R$(INC/expt) as a function of $\ln A_T$ with slopes slightly increasing with increasing incident energy and values equal to $+0.26$ and $+0.29$ for, respectively, positive and negative pions. In the case of our central collisions, the same feature has been observed with a slightly better linear fit for π^+ than for π^-. At $T_{\text{lab}}=800$ MeV, the corresponding slopes are 0.23 and 0.27 for π^+ and π^-, respectively (reaching 0.25 and 0.29 at $T_{\text{lab}}=1600$ MeV). Our results are thus in good agreement with the analysis of Ref. 22.

Experimental and INC π^+/π^- multiplicity ratios $R(\pi^+/\pi^-)$ are compared in Table X. The decrease of experimental $R(\pi^+/\pi^-)$ with the target mass is consistent with α-nucleus results[22] at 200, 400, 600, and 800 A MeV/nucleon. This target mass dependence is observed at the two incident energies and for the INC calculated $R(\pi^+/\pi^-)$ ratio. The theoretical $R(\pi^+/\pi^-)$ ratios overestimate the experimental values by, respectively, 80% and 40% at 800 and 1600 MeV. The fact that these $R(\pi^+/\pi^-)$ ratios are not well described by INC simulations for all targets was already pointed out in our analysis of the peripheral collisions. Such a behavior is quite different from the analysis of inclusive data.[14] It might be due to the fact that in the present data a better selection on impact parameter is achieved so that multiple collisions are more probable and charge exchange of both the nucleon and pion becomes more important. In addition, particles emitted in a more restricted phase space are presently analyzed. A linear dependence of $\ln R(\pi^+/\pi^-)$ in function of $\ln A_T$ is observed in our data. The slopes are -0.27 and -0.21 for, respectively, 800 and 1600 MeV incident energies, which has to be compared with -0.24 and -0.23 for INC predictions. The

TABLE VIII. Experimental and predicted pion mean multiplicities for central collisions. The calculated values are given for INC simulations (INC).

Incident energy		800 MeV			1600 MeV		
Target		C	Nb	Pb	C	Nb	Pb
	Expt	0.066	0.029	0.019	0.236	0.119	0.081
π^+	INC	0.133	0.099	0.069	0.284	0.206	0.197
	Expt	0.049	0.037	0.030	0.212	0.176	0.134
π^-	INC	0.058	0.061	0.062	0.169	0.213	0.258

TABLE IX. Ratio between INC predictions and experimental values of the pion mean multiplicities for central collisions.

Incident energy	800 MeV			1600 MeV		
Target	C	Nb	Pb	C	Nb	Pb
π^+	2.01±0.03	3.41±0.31	3.63±0.47	1.20±0.03	1.73±0.11	2.44±0.20
π^-	1.18±0.05	1.69±0.12	2.07±0.28	0.79±0.02	1.21±0.08	1.92±0.14

linear relationship is not as well satisfied theoretically as experimentally.

2. *Dispersion versus mean value of the multiplicity distributions*

In heavy-ion collision physics, a lot of activity has been devoted to studying of the pion multiplicity distribution in order to find any deviation from a Poisson distribution. Gyulassy and Kauffman[31] suggested that, at a given impact parameter, any deviation from a Poisson distribution might be a signature of a coherent effect. However, no deviation was found either in the Berkeley streamer chamber data for the Ar+KCl central collisions measured at 1.8A GeV (Rev. 32) or in the Dubna "semicentral" collisions at 3.66A GeV.[33] For the present experimental results, the dispersion is plotted as a function of the average multiplicity in Fig. 8 for peripheral and central collisions. The linear dependence expected from a Poisson distribution is generally observed except for mean multiplicities larger than 0.2, where deviations start to show up. No obvious explanation has been found for such a behavior.

V. CONCLUSIONS

Protonlike particles (free protons and protons bound in light fragments) and multiplicity distributions of both positively and negatively charged pions have been measured in proton-nucleus interactions at 800 and 1600 MeV incident energies. For that purpose the pictorial drift chamber of the large solid-angle DIOGENE detector has been used. It allows to sort out the events in two sets by means of a selection on the pseudoproton multiplicity: peripheral collisions $b_r \approx 0.7-0.9$ ($b_r = b/b_{\max}$) and central collisions $b_r \approx 0.5$.

As for the α-induced reactions studied with DIOGENE, the Liege INC code reproduces fairly well the protonlike multiplicity distribution for a light target such as C at both 0.8 and 1.6 GeV incident energies, while it overpredicts the protonlike cross sections for large multiplicities for heavier targets, the discrepancies being the largest for the Pb target.

The π^+ and π^- multiplicity distributions exhibit the following features:

For peripheral collisions it has been shown that the π^+ mean multiplicity decreases from a carbon to a lead target, but with a rate smaller at 1600 MeV than at 800 MeV. The π^- mean multiplicity displays a very weak target dependence, being almost constant from carbon to lead at 800 MeV and having a slight tendency to increase at 1600 MeV. The INC calculations reproduce only the mean π^- multiplicities at 1600 MeV, while at 800 MeV they overestimate the experimental data by a factor which varies from 1.2 to 2 from a carbon to a lead target. In contrast, the mean π^- multiplicities are generally underestimated. The INC π^+/π^- multiplicity ratios are twice as large as the experimental ones.

For central collisions the experimental mean π^+ and π^- multiplicities decrease from carbon to lead for both incident energies. The rate of decrease is smaller for π^- than for π^+ and does not depend on incident energy. The comparison with INC predictions shows that the theory overestimates the π^+ mean multiplicities, the discrepancy being the largest at the lower incident energy and for the heavier targets. For the π^- mean multiplicities, the cascade values are higher than the experimental values for all targets at 800 MeV, while at 1600 MeV the theory gives a value 20% lower than the experimental data for carbon and a value twice as large as the observed one for Pb.

The π^+/π^- multiplicity ratios for peripheral collisions are overestimated by about a factor of 2 for all targets by the INC calculations. For central collisions the calculated ratios are larger by a factor of 1.8 at 800 MeV and 1.4 at 1600 MeV.

The general observation that INC provides too large

TABLE X. π^+/π^- ratio of mean multiplicities for central collisions: experimental values, INC predicted value, and ratio R_{10} between INC and experimental values.

Incident energy	800 MeV			1600 MeV		
Target	C	Nb	Pb	C	Nb	Pb
Expt	1.35±0.01	0.78±0.02	0.63±0.01	1.11±0.01	0.68±0.01	0.60±0.01
INC	2.29±0.05	1.62±0.10	1.11±0.09	1.68±0.02	0.97±0.04	0.76±0.03
R_{10}	1.70±0.04	2.08±0.13	1.76±0.14	1.51±0.08	1.43±0.05	1.27±0.06

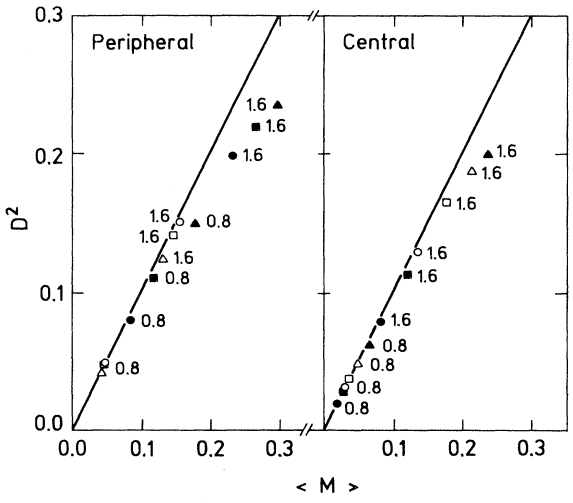

FIG. 8. Experimental values of the dispersion D^2 as a function of the average multiplicity of pions for peripheral (left) and central (right) collisions. The solid and open symbols correspond, respectively, to positively and negatively charged pions. Triangles, squares, and circles correspond respectively to C, Nb, and Pb targets. The numbers are the incident energies in GeV. The straight line is the function $D^2 = \langle M \rangle$.

mean multiplicities for heavy targets is consistent with the fact that INC misses some pion absorption.[34–36] In the case of α-induced reactions studied with DIOGENE, there was always some ambiguity about the origin of the discrepancies since, in this case, some compression occurs in these reactions. In the present experiment, no compression is about to occur in the reaction process. Thus the lack of compression in the INC cannot be responsible for the observed discrepancies between experiment and calculations. The fact that the experimental π^+/π^- multiplicity ratios disagree with the cascade values is quite new as compared to the analysis of the 730-MeV inclusive data. It might reflect that, with the impact parameter selection, the number of nucleon-nucleon collisions is under better control and that a process such as charge exchange or the isospin dependence of the elementary cross sections is not described precisely enough, all these effects being averaged out for inclusive cross sections. It may also be due to the fact that in the present work we are using a different phase space as the DIOGENE acceptance requires that the particles be emitted at large angles with high enough energies.

The present work corresponds to basic data obtained with an elementary probe and should be used to check theories developed for heavy-ion collisions to be sure that they are able to reproduce the global observables in a case where compression is absent.

ACKNOWLEDGMENTS

Special acknowledgments are due to the DPhN/ME technical staff whose support during the experiment was essential. Special thanks are due to F. Lepage and D. Bunel of DPhN and LNS.

*Present address: LNS, CEN Saclay, 91191 Gif-sur-Yvette Cedex, France.
†Present address: University of Heidelberg, Philosophenweg 12, D-6900 Heidelberg, RFA.
‡Present address: DPhN, CEN Saclay, 91191 Gif-sur-Yvette Cedex, France.

[1]E. Baron, S. Cooperstein, and S. Kahana, Nucl. Phys. **A440**, 744 (1985).
[2]J. Cugnon, T. Mizutani, and J. Vandermeulen, Nucl. Phys. **A352**, 505 (1981); M. Cahay, J. Cugnon, and J. Vandermeulen, *ibid.* **A411**, 524 (1983); J. Cugnon, La matière nucléaire dans tous ses ètats, Ecole Joliot Curie 1985, IN2P3 eds, (1985), p. 91.
[3]R. Stock *et al.*, Phys. Rev. Lett. **49**, 1236 (1982); R. Stock, Phys. Rep. **135**, 259 (1986) and references therein.
[4]J. W. Harris *et al.*, Phys. Rev. Lett. **58**, 463 (1987); in Proceedings of the 2nd Conference on the Intersections between Particle and Nuclear Physics, Lake Louise, Canada, 1986 (unpublished).
[5]J. J. Molitoris, H. Stöcker, and B. L. Winer, Phys. Rev. C **36**, 220 (1987).
[6]G. Bertsch, H. Kruse, and S. Das Gupta, Phys. Rev. C **29**, 673 (1984).
[7]H. Kruse, B. V. Jacak, and H. Stöcker, Phys. Rev. Lett. **54**, 289 (1985).
[8]C. Gale, Phys. Rev. C **36**, 2152 (1987).
[9]J. Aichelin, A. Rosenhauer, G. Peilert, H. Stoecker, and W. Greiner, Phys. Rev. Lett. **58**, 463 (1987).
[10]B. ter Haar and R. Malfliet, Phy. Rev. C **36**, 1611 (1987); B. ter Haar and R. Malfliet, Phys. Rep. **149**, 207 (1987).
[11]J. Cugnon, A. Lejeune, and P. Grangé, Phys. Rev. C **35**, 861 (1987).
[12]I. M. Mishustin, F. Myrher, and P. J. Siemens, Phys. Lett. **95B**, 361 (1980).
[13]P. J. Siemens, M. Soyeur, G. D. White, L. J. Lantto, and K. T. R. Davies, Phys. Rev. C **40**, 2641 (1989).
[14]J. Cugnon and M.-C. Lemaire, Nucl. Phys. **A489**, 781 (1988).
[15]D. R. F. Cochran, P. N. Dean, P. A. M. Gram, E. A. Knapp, E. R. Martin, D. E. Nagle, R. B. Perkins, W. J. Shlaer, H. A. Thiessen, and E. D. Theriot, Phys. Rev. D **6**, 3085 (1972).
[16]J. F. Crawford, M. Daum, G. H. Eaton, R. Frosch, H. Hirschmann, R. Horisberger, J. W. McCulloch, E. Steiner, R. Hausammann, R. Hess, and D. Werren, Phys. Rev. C **22**, 1184 (1980).
[17]L. Bimbot, V. Bellini, M. Bolore, X. Charlot, C. Guet, J. M. Hisleur, J. C. Jourdain, J. Julien, P. Kristiansson, G. Lanzano, B. Million, A. Oskarsson, A. Palmeri, G. S. Pappalardo, J. Poitou, F. Reide, and N. Willis, Nucl. Phys. **A440**, 636 (1985).
[18]N. J. DiGiacomo, M. R. Clover, R. M. DeVries, J. C. Dousse, J. S. Kapustinsky, P. L. McGaughey, W. E. Sondheim, J. W. Sunier, M. Buenerd, and D. Lebrun, Phys. Rev. C **31**, 292 (1985).
[19]V. V. Abaev, E. P. Fedorova-Koval, A. B. Gridnev, V. P.

Koptev, S. P. Kruglov, Yu A Malov, G. V. Scherbakov, I. I. Strakovsky, and N. A. Tarasov, J. Phys. G **14**, 903 (1988).

[20]J. P. Alard, J. Arnold, J. Augerat, R. Babinet, N. Bastid, F. Brochard, J. P. Costilhes, M. Crouau, N. DeMarco, M. Drouet, P. Dupieux, H. Fanet, Z. Fodor, L. Fraysse, J. Girard, P. Gorodetzky, J. Gosset, C. Laspalles, M. C. Lemaire, D. L'Hôte, B. Lucas, G. Montarou, A. Papineau, M. J. Parizet, J. Poitou, C. Racca, W. Schimmerling, J. C. Tamain, Y. Terrien, J. Valero, and O. Vallette, Nucl. Instrum. Methods **A261**, 379 (1987).

[21]C. Racca, Thèse d'état, Université de Strasbourg, 1987.

[22]D. L'Hôte, Thèse d'état, Université de Paris-Sud, 1987.

[23]D. L'Hôte, J. P. Alard, J. Augerat, R. Babinet, F. Brochard, Z. Fodor, L. Fraysse, J. Girard, P. Gorodetzky, J. Gosset, C. Laspalles, M. C. Lemaire, B. Lucas, G. Montarou, M. J. Parizet, J. Poitou, C. Racca, W. Schimmerling, J. C. Tamain, Y. Terrien, J. Valero, J. Cugnon, and Vandermeulen, Phys. Lett. **198**, 139 (1987).

[24]J. Poitou, Nucl. Instrum. Methods **A217**, 373 (1983).

[25]C. Cavata, thèse, Université de Paris-Sud, 1989, Report No. CEA-N-2629, 1990 (unpublished).

[26]E. J. Moniz, I. Sick, R. R. Witney, J. R. Ficenec, R. D. Kephart, and W. P. Trower, Phys. Rev. Lett. **26**, 445 (1971).

[27]J. Jaros, A. Wagner, L. Anderson, O. Chamberlain, R. Z. Fuzesy, J. Gallup, W. Gorn, L. Schroeder, S. Shannon, G. Shapiro, and H. Steiner, Phys. Rev. C **18**, 2273 (1978).

[28]L. Ray, Phys. Rev. C **20**, 1857 (1979).

[29]Alma-Ata-Baku-Budapest-Bucharest-Varna-Warsaw-Dubna-Erevan - Krakow - Moscow - Prague - Sofia - Tashkent-Tbilisi - Ulan-Bator Collaboration, Yad. Fiz. **30**, 1590 (1979) [Sov. J. Nucl. Phys. **30**, 824 (1979)]; SKM-200 Collaboration, Nucl. Phys. **A362**, 376 (1981).

[30]M. M. Sternheim and R. R. Silbar, Phys. Rev. D **6**, 3117 (1972).

[31]M. Gyulassy and S. K. Kauffmann, Phys. Rev. Lett. **40**, 298 (1978).

[32]R. Stock, GSI Report No. GSI-85-17, 1985 (unpublished).

[33]R. Swed, Report No. LBL-12652, 1981 (unpublished), p. 371.

[34]R. D. McKeown, S. J. Sanders, J. P. Schiffer, H. E. Jackson, M. Paul, J. R. Specht, E. J. Stephenson, R. P. Redwine, and R. E. Segel, Phys. Rev. C **24**, 211 (1981).

[35]G. Backenstoss, M. Izycki, P. Salvisberg, M. Steinacher, P. Weber, H. J. Weye, S. Cierjacks, B. Rzehorz, H. Ulrich, M. Furié, T. Petkovic, and N. Simicevie, Phys. Rev. Lett. **59**, 767 (1987).

[36]L. L. Salcedo, E. Oset, M. J. Vicente-Vacas, and C. Garcia-Recio, Nucl. Phys. **A484**, 557 (1988).